Research Article

Influence of Nanoparticle Size Distributions on the (in)Stability and Rheology of Colloidal SiO₂ Dispersions and HPAM/SiO₂ Nanofluid Hybrids

Maje Alhaji Haruna[1*] (ID) **, Saminu Musa Magami**[2] (ID)

[1]School of Chemical and Process Engineering, University of Leeds, Leeds, United Kingdom
[2]Wigan, Greater Manchester, United Kingdom
 Email: majeharuna@gmail.com

Abstract: This study investigated the relationship between variations in the size distribution and the specific surface area of SiO₂ nanoparticles and the in(stability) and rheology of their colloidal dispersions and their resulting silica-poly(acrylamide) hybrids. Thus, SiO₂ nanoparticles with size distribution in the range 40-173 nm, corresponding to 70-26 m²/g of specific surface area, were used in the studies. The results show a correlation between the average particle size distribution/the specific-surface area of silica nanoparticles with the in(stability) and the rheology of their dispersions, such that an increase in the particle size distribution from 40 to 173 nm corresponds to a decrease in dispersion instability index from 0.913 to 0.112. However, in the silica-poly(acrylamide) hybrids, a change in the particle size distribution from 40 to 173 nm corresponds to an increase in the nanofluid instability index from 0.1913 to 0.929. In the hybrid materials, interactions between polymer chains and nanoparticles lead to size-induced stability and rheological behaviour, such that the broadening of the FTIR peak around 1,000 cm⁻¹ in the nanohybrids was related to an Si-O-H bending vibration that arose because of dominating hydrogen bonding arising from the interaction of the hydroxyl groups and the amide groups in the polymer. The rheological characteristics of the hybrid nanofluids show that the relative viscosity and shear sensitivity of the colloidal dispersions or their hybrids can be tailored by the average particle size distribution of the nanoparticles.

Keywords: silica, nanoparticles, poly(acrylamide), in(stability), rheology

1. Introduction

Nanofluids are essentially produced by suspending nano-sized particles or composites in a fluid medium that may or may not contain surfactants, macromolecules, or ionic salts.[1,2] The essential characteristics of many nanofluid variants are governed by a range of physical, chemical, thermal, and rheological factors such as solid volume fraction, viscosity, conductivity, heat transfer coefficients, the concentration of materials or their type, structure, size, shape and concentration, distributions and size of constituent nano-particulates.[3-5] Therefore, studies on nanofluids typically concern providing an account of how such properties are influenced, measured, and characterised.[6,7]

Many colloidal nanofluids have the potential for applications in a range of fields, including solar collectors/cells,[8] electrolyte membranes,[9] heat exchangers,[10,11] (micro)electronics,[12] computed tomography (CT) imaging,[13] drug release,[14]

dye removal,[15] enhanced oil recovery,[16,17] fire resistance,[18] flame retardance,[19] surface coatings,[20] photocatalysis,[21] and so on. Many of the materials are composed of purely inorganic materials stabilised in a liquid medium. This category includes dispersions of fullerene in water,[22] dispersions of silica in water,[23] and dispersions of carbon nanotubes in water.[24] Another category is that of organic-inorganic hybrids that have been fabricated with desired morphology and structure. Some of the well-reached examples are dispersions of polybenzimidazole/silica,[25] dispersions of polyimide/titanium dioxide,[26] and dispersions of polyvinyl alcohol/graphene oxide.[27]

The stability of colloidal nanoparticles or nanocomposite dispersions involves controlling how the dispersed particulates are suspended and dispersed, thus ensuring that nucleation and inter-particulate attractions/collisions are minimised.[28] Typically, stability is achieved by the formation of an electrical double-layer (zeta potential) that is defined as the potential difference between the dispersion medium and the stationary layer of fluid attached to the nanoparticles.[29] It can also be attributed to a steric hindrance phenomenon that is typically caused by the use of suitable macromolecules in the formulation. The presence of macromolecular polymer species that can cause covalent functionalisation in the nanofluids[30] or ionic salts that can affect charge separation and distribution are other factors.[31] Stability or lack of it in nanofluids can be studied by elementary sedimentation techniques which evaluate how the dispersed nanoparticles remain suspended or become settled with time.[32]

The viscosity of colloidal nanofluids is considered to be an important property that governs the application of dispersions.[33] Size distribution of the nanoparticles used in nanofluids is also an essential parameter.[34] Despite this knowledge, some researchers argue that the number of studies carried out on the effect of particle size on viscosity of nanofluids is inadequate.[35] For the majority of such reports, it has been argued that the particle size range considered in the studies was limited.[11] Thus, any attempt that underpins how the viscosity of colloidal dispersions affects performance properties such as concentration, volume fraction, stability, and hydrodynamics, becomes important.[36] Such importance cannot be overemphasised since many studies rely on theoretical modelling where often the effect of viscosities on material behaviour is underestimated.[37]

In this work, experimental studies were undertaken with the view of understanding how the average particle size distribution (APS) of SiO_2 nanoparticles and their specific surface area (SSA) have an effect on the viscosity of the nanofluids and their resulting polymer/nanoparticle hybrids. In addition, such variants were studied on how they affect the (in)stability of the colloidal silica dispersions or their resulting polymer/nanoparticle hybrids.

2. Materials and methods

The colloidal silica samples used in this study were obtained from the University of Leeds, Nouryon, the Merck Group, and CWK Bad Köstritz. Each material was an aqueous solution of approximately 50% solids. The materials were studied for their average particle distribution and zeta potential before they were used in the preparation of the test samples. Polyacrylamide was obtained from SNF FLOERGER, France, with a relative density of 0.9 g/cm^3 and a molecular weight of 3-5 MDa.

3. Experimental

A Dynamic Light Scattering (DLS) technique, using a Malvern Zeta Sizer Nano ZS, was used as the basis for the particle size studies and zeta potential measurements. Dilute dispersions of the samples were placed in polystyrene cuvettes and DTS 1060 capillary cells, respectively, for the particle size studies and zeta potential measurements.

The specific surface area of the silica particles was determined by means of an Accelerated Surface Area and Porosimetry System 2020, utilising a liquid nitrogen flow. Each dispersion was priori dried in an oven at 85 °C overnight in order to obtain a solid residue. Each sample was then placed in the heating chamber of the instrument, where a flask was connected to a degassing mechanism, leading to a further drying of the samples for 3 hours at 120 °C. After reaching a steady vacuum, nitrogen gas was pumped into the flask following which the specific surface area was measured.

SEM microscopy was carried out using a Joel JSM-6610LV scanning electron microscope, coupled with an Oxford Instruments X-max80 EDS spectrometer. A drop of each diluted material was added to an SEM stub, to which a strip

of copper tape was priori attached. Each stub was then allowed to dry before it was coated with a 30 nm layer of gold, using a Quorum Q150RS device.

The stability studies were carried out to investigate and understand the nature of sedimentation and flocculation of the samples using a LUMiSizer (Lum GmbH, Germany), a dispersion analyser centrifuge that measures the near-infrared light transmission under the influence of centrifugal force. For each sample, 0.5 mL was pipetted in a polycarbonate capillary cell and sealed carefully with a sealing cap. The sample tubes were inserted into the equipment and centrifuged for about 50 min at 2,600 rpm (light factor 1, 25 °C, 870 nm NIRLED). The software attached to the instrument was used to record the real-time transmission profiles at designated time intervals.

The rheological studies were carried out using a Physica MCR 301 rheometer (Anton Paar, Austria). To control the shear rate across the radius, a cone and plate geometry was chosen to measure the viscosity. In this, the measuring gap was pre-set to the standard 0.098 mm value as set out by the instrument manufacturer. The experimental temperature was set at 25 °C, controlled by the "TC30" temperature controller system which can manage the sample temperature from 0 up to 1,000 °C. During each measurement, approximately 0.7 mL of the sample was deposited onto the device's lower geometry plate. Prior to the measurements, the set-up was calibrated using standard oil and pure water to test the accuracy of the rheometer. The results were compared with the manufacturer's reliable data. All experiments were carried out under a shear-rate-controlled mode.

4. Results and discussions
4.1 *Characteristics of the various colloidal silica materials*

Many physical-chemical properties of nanofluids depend on the size and the morphological state or surface of their constituent nanoparticles.[38] Therefore, at first, an in-depth characterisation of the various nanomaterials considered for this study was undertaken. The average particle size distribution, zeta potential, and microstructure were studied to determine the dispersion characteristics. Table 1 shows a summary of the characteristic average particle size distribution (nm), polydispersity index (PDI), zeta potential (mV), and specific surface area (m^2/g) of the various silica dispersions or their particles. The plots associated with the adsorption/desorption properties of the nanoparticle powders, from which the specific surface area data was obtained, are presented as Figure 1.

Table 1. Characteristic average particle size distribution (nm), polydispersity index (PDI), zeta potential (mV), and specific surface area (m^2/g) of the various silica dispersions or their particles

Sample reference	Average particle size (nm)	PDI	Zeta potential (mV)	SSA (m^2/g)
SiO$_2$ (172.5 nm)	172.5 ± 2.1	0.18 ± 0.01	-52.7 ± 1.0	26.2 ± 4.01
SiO$_2$ (116.5 nm)	116.5 ± 3.0	0.11 ± 0.02	-48.2 ± 1.6	34.1 ± 6.7
SiO$_2$ (86.9 nm)	86.9 ± 3.8	0.091 ± 0.03	-47.8 ± 0.9	38.5 ± 4.01
SiO$_2$ (86.8 nm)	86.8 ± 1.8	0.083 ± 0.001	-46.6 ± 0.5	51.9 ± 7.01
SiO$_2$ (40.6 nm)	40.6 ± 4.2	0.089 ± 0.04	-41.4 ± 1.7	70.1 ± 6.1

The particle size distribution for the various SiO$_2$ samples is shown in Figure 2. In each case, a monomodal distribution of the particles is seen. This also indicated that for each material, the primary particles and their size distributions are determined. Hence, the poly dispersity index (PDI) of all the colloidal materials was < 0.2. For the individual samples, a correlation between the size distribution and the SSA is demonstrated by comparing the data given in Table 1. This shows that the higher the average size distribution, the lower the SSA. In these, range of SSA values are

therefore seen, with the larger SSA values corresponding to silica particles more porous than those with low SSA. The zeta potential values associated with the SiO_2 variants are shown in Figure 3. All the colloidal silica dispersions exhibit a zeta potential in the range that is appropriate for good dispersion stability. Thus, in nanofluids, having zeta potential values in the range 40-60 mV is believed to correspond to excellent dispersion stability.[39]
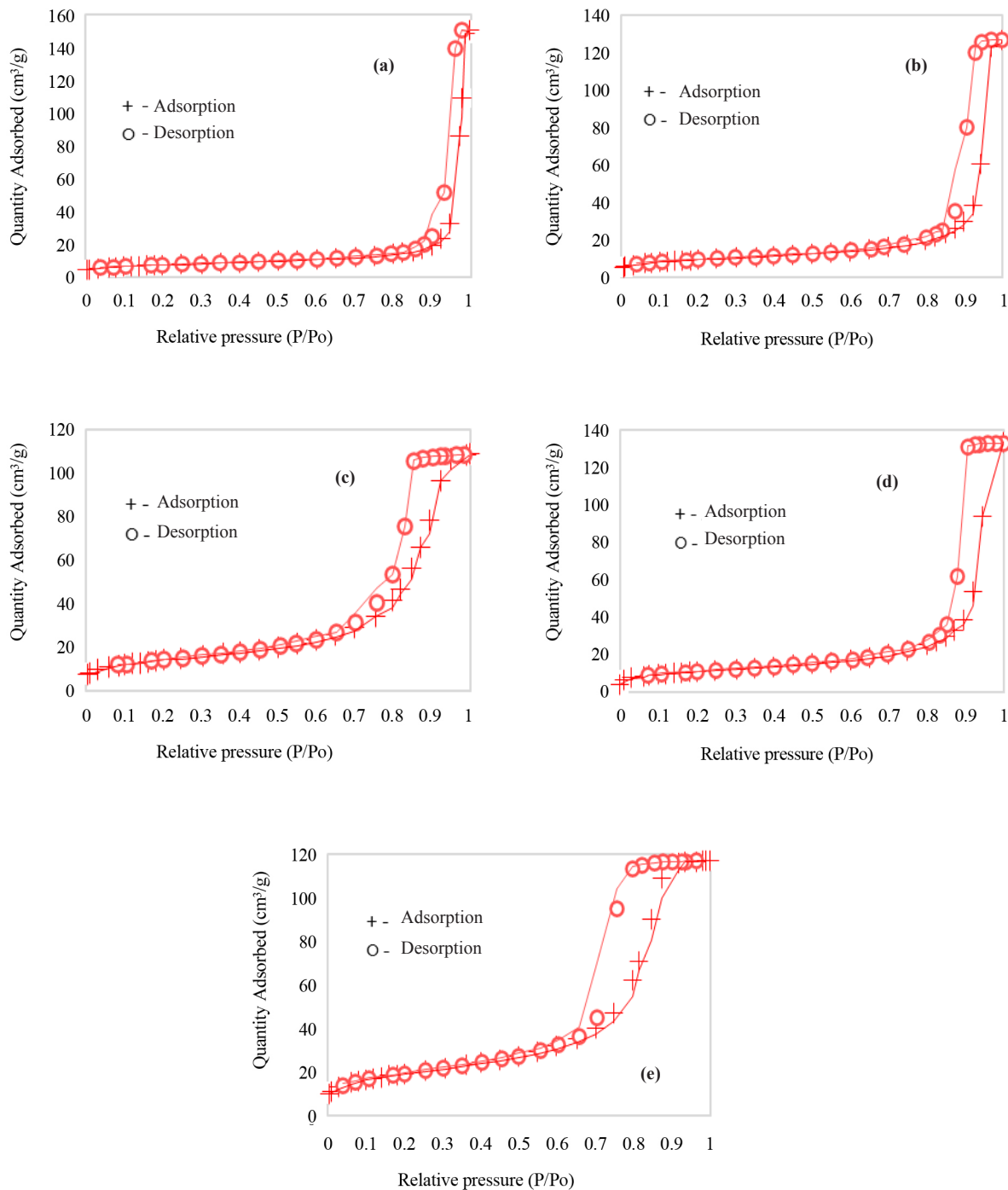

Figure 1. Plots associated with the adsorption/desorption properties of the nanoparticle powders from which specific surface area values were determined: (a) SiO_2 (172.5 nm), (b) SiO_2 (116.5 nm), (c) SiO_2 (86.9 nm), (d) SiO_2 (86.8 nm) and (e) SiO_2 (40.6 nm)
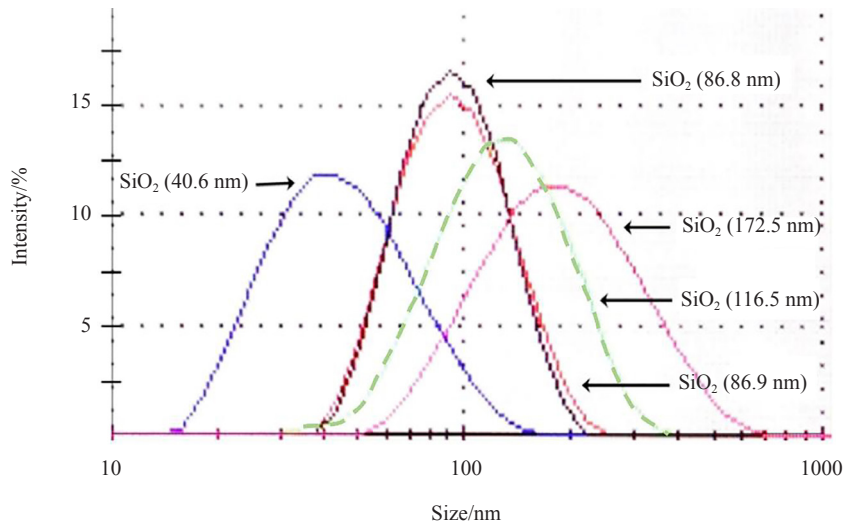
Figure 2. Particle size distribution for the various SiO$_2$ samples, with the average particle size indicated for each material
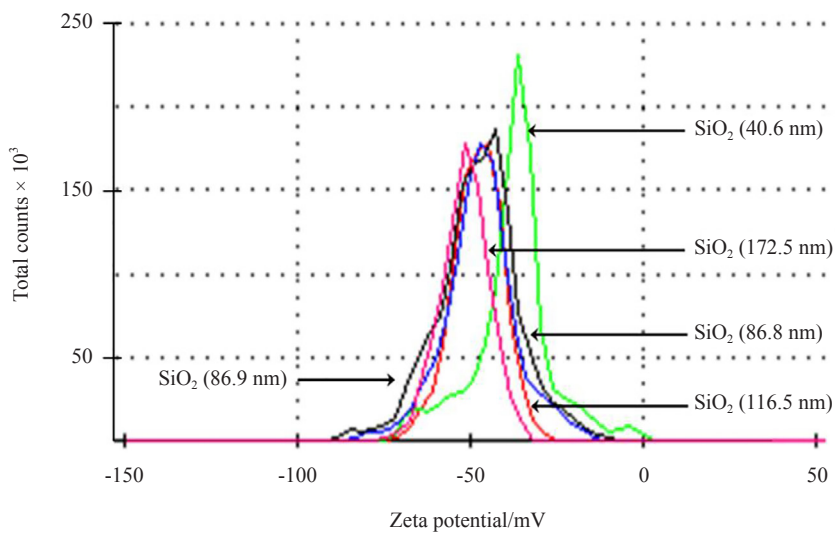

Figure 3. Zeta potential plots for the various SiO$_2$ samples, with the corresponding average particle size indicated for each material

The morphological characterisation of nanoparticles or nanocomposites is important because it helps understand what the shape of individual particles is and essentially how uniform the shape is in the materials.[40] The surface morphology characteristics of the SiO$_2$ samples, obtained from SEM analyses, are represented in Figure 4. In all cases, the morphologies show that the SiO$_2$ nanoparticles exhibit well defined spherical particles. In this, primary particles can be seen. Assessment of the sizes of the nanoparticles and their distribution shows good agreement with the data given in Figure 2, and summarised in Table 1. This also shows how well dispersed the colloidal dispersions were. In the SiO$_2$ (172 nm) colloidal silica material, a range of particle sizes can be seen. This material has a PDI value of 0.18, relatively the largest in all the materials studied. Again, a good correlation between the SEM images and the PDI values given in Table 1 can be seen.
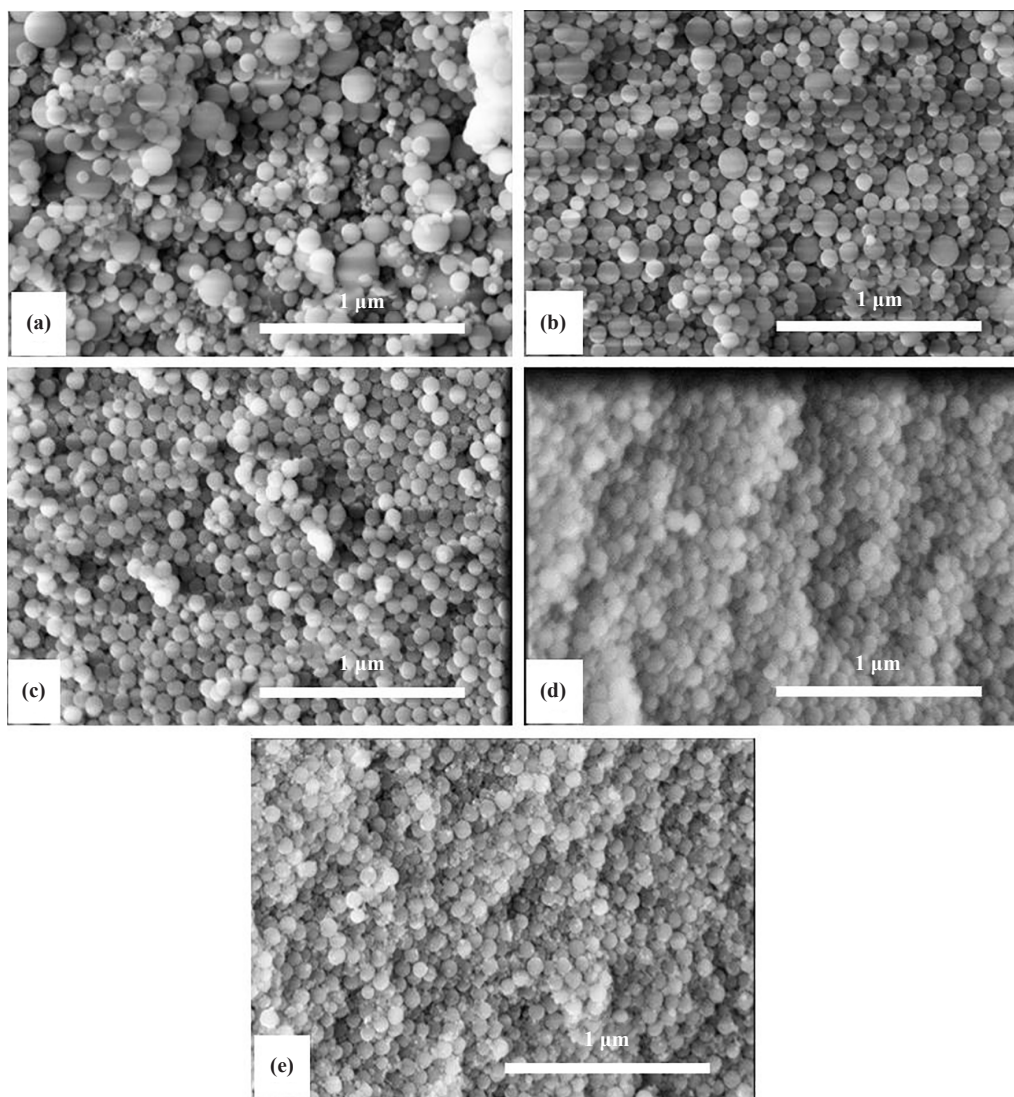
Figure 4. SEM images of the SiO$_2$ nanoparticles: (a) SiO$_2$ (172.5 nm), (b) SiO$_2$ (116.5 nm), (c) SiO$_2$ (86.9 nm), (d) SiO$_2$ (86.8 nm) and (e) SiO$_2$ (40.6 nm)

4.2 *Interactions in the SiO$_2$/HPAM nanohybrids*

The FT-IR spectra obtained from the SiO$_2$ nanoparticles, the HPAM material used in formulation and the SiO$_2$/HPAM nanohybrids are presented in Figure 5. The spectral peaks seen at around 1,200 cm^{-1} arise due to Si-O-Si asymmetric stretching. Those observed around 800 and 490 cm^{-1} are associated with Si-O-Si symmetric stretching and bending. The presence of the key silica functional groups and their persistence in the SiO$_2$/HPAM nanohybrids show that a successful fabrication has taken place. The broadening of the peak around 1,000 cm^{-1} in the nanohybrids can also be an indication of typical Si-O-H bending vibration that generally arises because of hydrogen bonding events becoming significant and arising from interaction of the hydroxyl groups and the amide groups in the polymer.[30,41] In addition, the appearance of the peak in the vicinity 3,200 to 3,700 cm^{-1} indicates the vibration of -OH, SiO-H and N-H groups. Thus, the overall strong functional group interactions seen between the SiO$_2$ and the HPAM material are the results of the increased viscosity in the nanofluids relative to the colloidal dispersions, as discussed in the next sections.
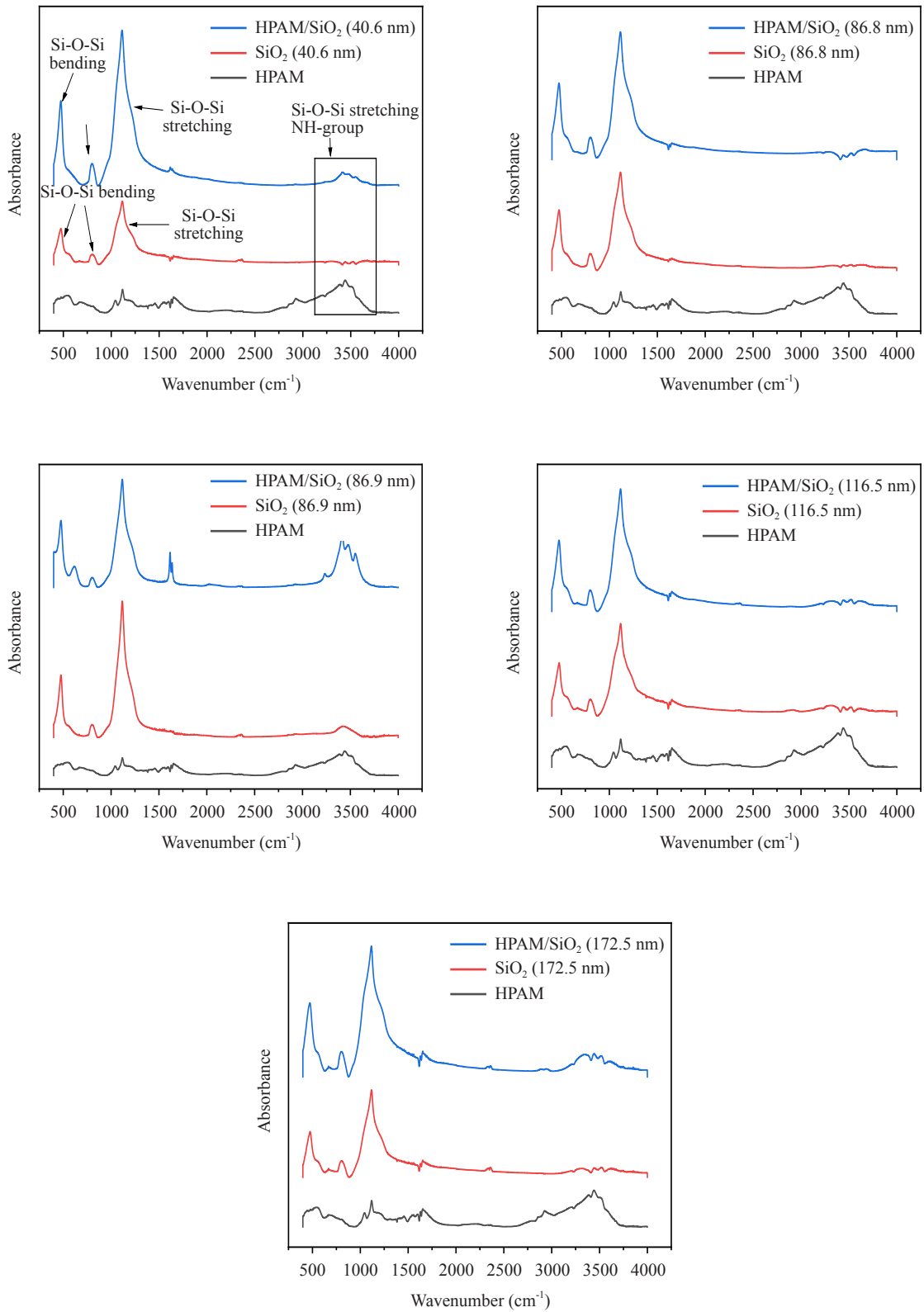
Figure 5. FT-IR spectra obtained from the SiO$_2$ nanoparticles, the HPAM material used in formulation and the SiO$_2$/HPAM nanohybrids

4.3 *Effect of particle size distribution on the (in)stability characteristics of the silica dispersions*

Figure 6 and Figure 7 show the plots of the instability index of the aqueous dispersions of the SiO_2 nanoparticles and how these relate to the average particle size and the specific surface area. The highest instability observed in the dispersion with the lowest average particle size distribution arises due to its large specific surface area. In this composition, the particles have a low thermodynamic stability and tend to agglomerate over time-hence the greatest instability index over time.[42] Furthermore, the particles in the colloidal silica dispersions are governed by Brownian motion, which is considered to be a diffusion process that is governed by the Stokes-Einstein equation.[43] Brownian motion is a characteristic of the particles in the colloidal system and is affected by the size of the particles and the viscosity of the medium. Thus, particle motion in the dispersion becomes greater when the average particle size is higher. Hence, as the size of the silica particles increases, the Brownian movement becomes less.[44]
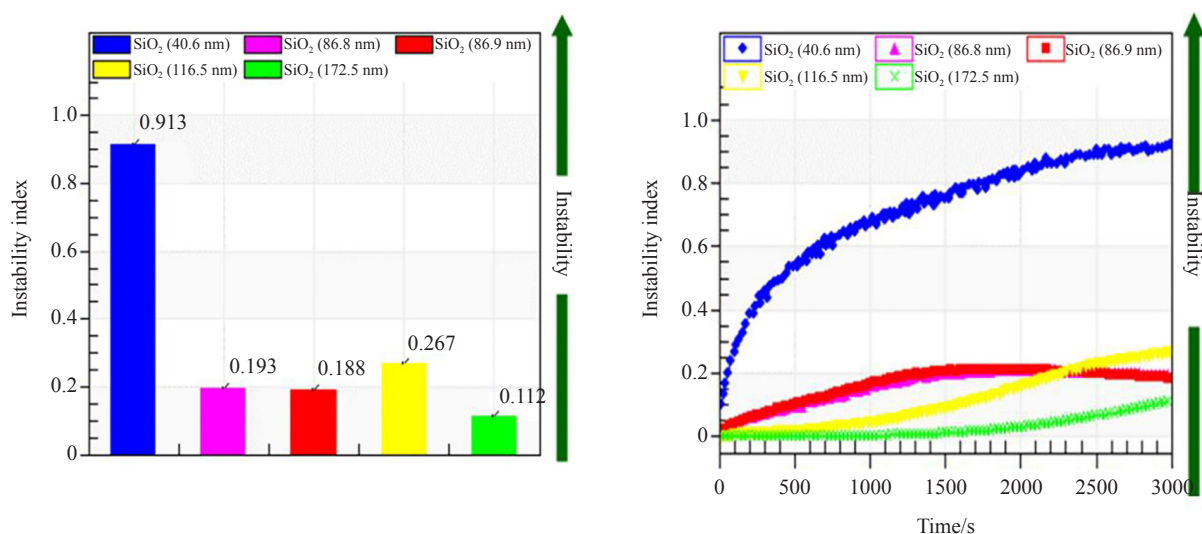

Figure 6. (L) Instability index values of the aqueous dispersions of the SiO_2 nanoparticles after 2,500 s and (R) Variation of the instability index with time in the aqueous dispersions of the SiO_2 nanoparticles
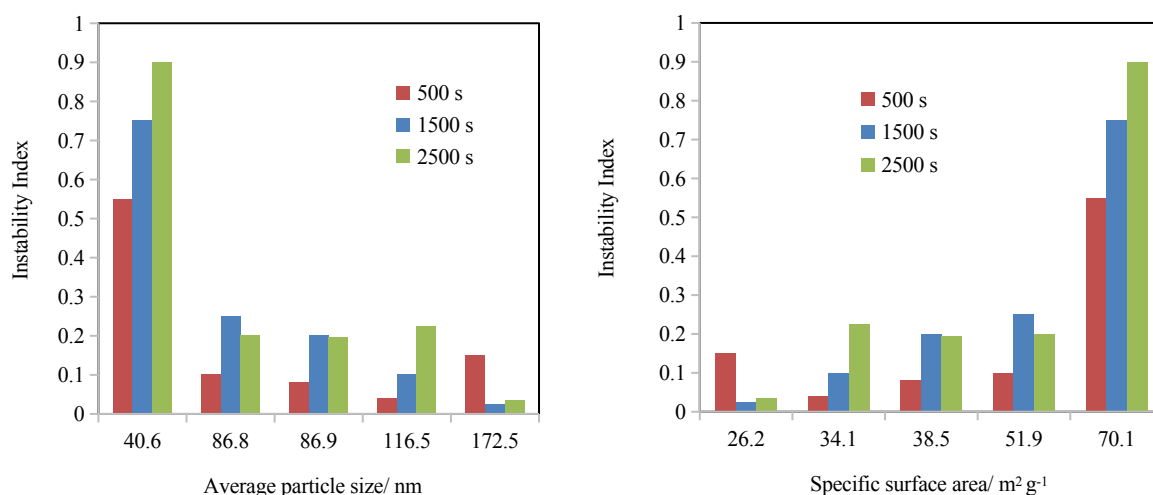

Figure 7. Comparison of the instability index values of the aqueous dispersions of the SiO_2 nanoparticles at different times: (L) as a function of the average particle size and (R) as a function of the specific surface area

A comparison of the DLS characteristics of the nanoparticle dispersion presented in Table 1, with the overall results given in Figure 6 and Figure 7, clearly shows the limitation of the DLS technique, since it was not able to carefully examine the roles that possible artifacts such as aggregation and sedimentation of particles play during these measurements.[45] Additionally, the DLS measurements are limited in observing how these effects occur within experimental times. Thus, testing the instability index becomes important in understanding the effects of particle size or particle morphology on sedimentation in dispersed systems.

4.4 *Effects of the poly(acrylamide) polymer on the silica particles and their (in)stability characteristics as per their size distribution*

The dispersion stability of the SiO_2/HPAM nanohybrids was also investigated using the lumisizer technique in order to understand how the APS distribution of the nanoparticles affects the sedimentation behaviour. Thus, the instability characteristics of the colloidal nanoparticle dispersions are presented in Figure 8 and Figure 9. These relate to the associated light transmission properties across the test tubes of the SiO_2/HPAM nanohybrids, obtained from the lumisizer studies.

The trends seen in Figure 8 and Figure 9 show that the instability index is higher where the average particle size of the silica nanoparticles is higher, and lower with a decreased average particle size. When the APS is higher, the resulting nanohybrids exhibit greater potential for sedimentation because of a higher open hybrid-bed structure which makes the material more sensitive to the applied centrifugal force. Figure 5 shows that the poly(acrylamide) polymer chains produce surface-modified silica nanoparticles. Such effects have been reported in SiO_2/HPAM,[46] SiO_2/Xanthan-Gum/HPAM[47] and SiO_2/Graphene-Oxide.[48] In another study, the colloidal dispersion of a specific SiO_2/HPAM showed improved dispersion stability compared to that of pure HPAM and neat SiO_2 dispersions.[49] In the current study, this means that interactions are formed between the polymer and the nanoparticles. The result of this interaction is that polymer-nanoparticles that are formed exhibit an overall size dependent stability characteristic.
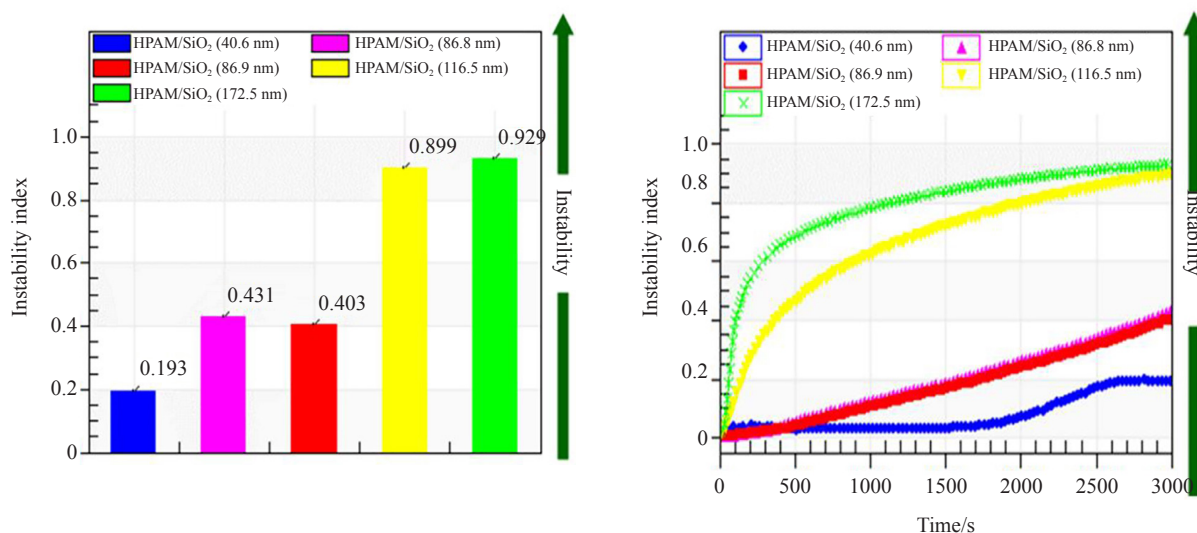

Figure 8. (L) Instability index values of the SiO_2/HPAM nanohybrids after 2,500 s, (R) Variation of the instability index with time in the SiO_2/HPAM nanohybrids

The overall effects observed in Figure 8 and Figure 9 are contrary to the traditional steric stability that the presence of polymers such as poly(3-cyanopropyl)methyl siloxane or poly(dimethysiloxane) offer in influencing the stability of colloidal dispersions. In these, it was thought that nitrile functional groups in the polymers adsorb onto the particle surface or protrude into the cobalt-based colloid to provide stabilisation.[50] Similar stabilisation has been reported where

surface modification of the silica nanoparticles is achieved by (3-glycidoxypropyl)trimethoxy silane species.[51] However, as the current results show, interaction between the SiO_2 and the HPAM persists resulting in an overall size dependent stability behaviour. Studies have established that HPAM chains become adsorbed on the surface of silica nanoparticles due to hydrogen bonding. This results in physical crosslinking between the silica particles and the polymeric chains of HPAM.[52]
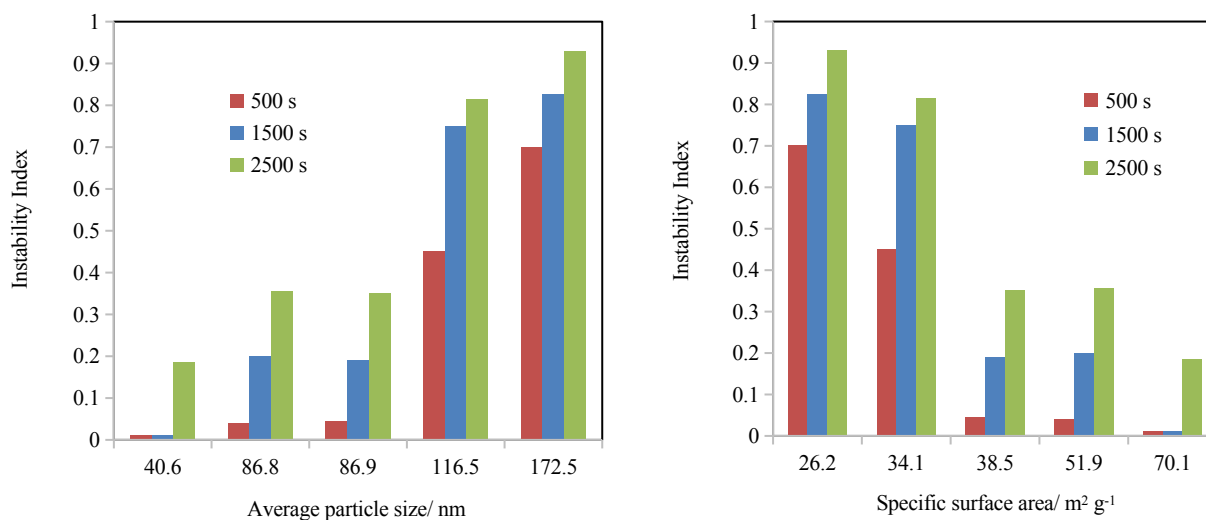

Figure 9. Comparison of the instability index values of the SiO_2/HPAM nanohybrids after at different time (L) as a function of the average particle size, (R) as a function of the specific surface area

4.5 *Effects of the poly(acrylamide) polymer on the silica particles and rheology*

The influences of the average particle size distribution of the SiO_2 nanoparticle on the shear sensitivity of the colloidal dispersions were examined at 25 °C. The results presented in Figure 10 show that the effective viscosity of the colloidal dispersions is a factor of the average particle size distribution of the nanoparticles. Thus, dispersions with higher APS distribution possess higher viscosity. These effects correlate well with a study where an increment in the relative viscosity of TiO_2-based dispersions was reported with an increase in the particle size distribution.[53] In addition, higher viscosities were observed where the particle size distribution was greater in some Al_2O_3-based and CuO-based aqueous dispersions.[54]

In Figure 10, when the average particle size distribution of the SiO_2 nanoparticles is increased from 40.6 to 172.5 nm, it is reasonable to consider that the nanoparticle volume fraction is increased. Thus, the colloidal SiO_2 dispersions with an overall lower APS distribution behaved as if their total particle concentration was lower. This effect therefore corresponds to reports on how the volume fraction of silver-based dispersions enhances the viscosity of the materials.[55]

The rheological characteristics of the HPAM/SiO_2 nanofluid hybrids are represented in Figure 11. These show that the shear viscosities of the nanofluid hybrids decrease first with an increase in shear rate, exhibiting shear thinning behaviour. Then, the viscosities approach a near constant value at a shear rate of 1,000 s^{-1}. The rate at which the viscosities decreased was greatest in the hybrid material that contained the SiO_2 nanoparticles with the highest average particle size (lowest specific surface area). This shows that the flow nature of the nanofluids is sensitive to the average particle size distribution. Figure 5 has described the nature of the bonding in the nanohybrid materials and how the interactions between the hydroxyl groups in the silica and the amide groups in the polymer arise through dominant hydrogen bonding. The trends in Figure 11 further show that the initial increase in viscosity, in all the nanohybrids relative to the neat-HPAM, was associated with increased inter-molecular interactions in the nanohybrids.
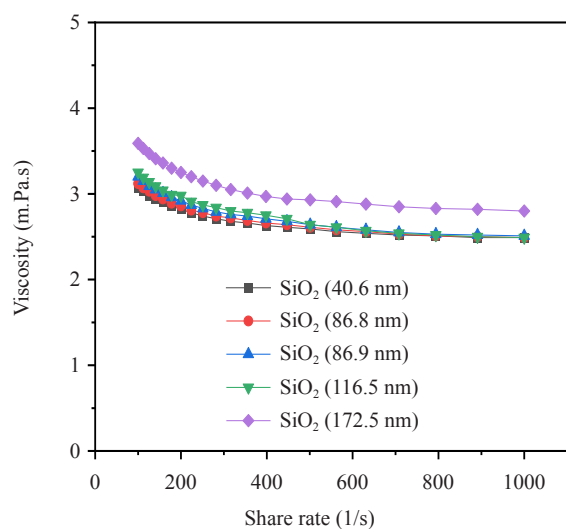
Figure 10. Flow characteristics of the aqueous dispersions of the SiO_2 nanoparticles
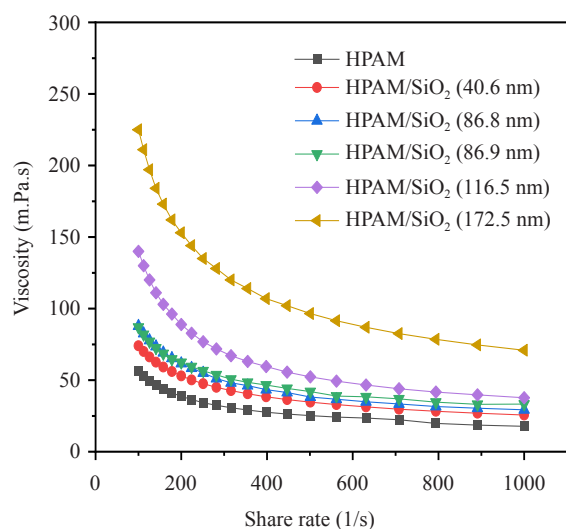

Figure 11. Flow characteristics of the HPAM/ SiO_2 nanofluids in comparison the HPAM polymeric material

5. Conclusions

This study demonstrated how HPAM/SiO_2 hybrid nanofluids can be prepared and evaluated for long term (in) stability and characteristic flow. In this, a range of techniques including DLS, lumisizer testing and rheology were employed. These show that a correlation exists between the average particle size distribution of SiO_2 nanoparticles or their specific surface area with the stability and rheology of their dispersions. It also shows that when HPAM/SiO_2 hybrid nanofluids are formed, the average particle size distribution of the SiO_2 nanoparticles also plays a key role on the stability and the rheology of the nanohybrids. In these, the organic-inorganic associations formed in the hybrids arise because of interactions largely between the hydroxyl groups in the silica and the amide groups in the polymer, through dominant hydrogen bonding. These lead to a size dependent stability and viscosity properties in the various materials. Thus, the overall results could be critical in understanding how colloidal stability is dictated in similar dispersions and

nanofluids and how macromolecular movements are enhanced or retarded by incorporating SiO$_2$ nanoparticles with specific particle size or specific surface area in polymer solutions.

Conflict of interest

The authors declare no competing financial interest.

References

[1] Bhanvase, B.; Barai, D. Introduction to Nanofluids. In *Nanofluids for Heat and Mass Transfer*; Bhanvase, B., Barai, D., Eds.; Academic Press, 2021; pp 3-42.

[2] Wong, K. V; De Leon, O. Applications of Nanofluids: Current and Future. *Adv. Mech. Eng*. **2010,** *2*, 519659.

[3] Mahbubul, I. M. Stability and Dispersion Characterization of Nanofluid. In *Micro and Nano Technologies; Mahbubul Characterization, Properties and Application of Nanofluid*; Mahbubul, I. M., Ed.; William Andrew Publishing, 2019; pp 47-112.

[4] Bhanvase, B.; Barai, D. *Electrical, Optical, and Tribological Properties of the Nanofluids*; Academic Press, 2021; pp 167-190.

[5] Bhanvase, B.; Barai, D. Laboratory-Scale Synthesis and Scale-up Challenges. In *Nanofluids for Heat and Mass Transfer*; Bhanvase, B., Barai, D. B., Eds.; Elsevier, 2021; pp 43-68.

[6] Meng, Q.; Magami, S. M. Metallic Powders for Composite Inks: Formulation, Application, and Characterization. *Res. J. Nanosci. Eng*. **2017,** *1*, 14-23.

[7] Alheshibri, M.; Elsayed, K.; Haladu, S. A.; Musa Magami, S.; Al Baroot, A.; Ercan, İ.; Ercan, F.; Manda, A.; Çevik, E.; Kayed, T. S.; et al. Synthesis of Ag Nanoparticles-Decorated on CNTs/TiO$_2$ Nanocomposite as Efficient Photocatalysts via Nanosecond Pulsed Laser Ablation. *Opt. Laser Technol*. **2022,** *155*, 108443.

[8] Farooqi, Z. H.; Butt, Z.; Begum, R.; Khan, S. R.; Sharif, A.; Ahmed, E. Poly(N-Isopropylacrylamide-Co-Methacrylic Acid) Microgel Stabilized Copper Nanoparticles for Catalytic Reduction of Nitrobenzene. *Mat. Sci.-Pol*. **2015,** *33*, 627-634.

[9] Mohamed, H. F. M.; Abdel-Hady, E. E.; Abdel-Moneim, M. M. Y.; Bakr, M. A. M.; Soliman, M. A. M.; Shehata, M. G. H.; Ismail, M. A. T. Effect of Al$_2$O$_3$ on Nanostructure and Ion Transport Properties of PVA/PEG/SSA Polymer Electrolyte Membrane. *Polymers (Basel)*. **2022,** *14*, 4029.

[10] Kumar, V.; Tiwari, A. K.; Ghosh, S. K. Application of Nanofluids in Plate Heat Exchanger: A Review. *Energy Convers. Manag*. **2015,** *105*, 1017-1036.

[11] Koca, H. D.; Doganay, S.; Turgut, A.; Tavman, I. H.; Saidur, R.; Mahbubul, I. M. Effect of Particle Size on the Viscosity of Nanofluids: A Review. *Renew. Sust. Energ. Rev*. **2018,** *82*, 1664-1674.

[12] Nilagiri Balasubramanian, K. B.; Ramesh, T. Role, Effect, and Influences of Micro and Nano-Fillers on Various Properties of Polymer Matrix Composites for Microelectronics: A Review. *Polym. Adv. Technol*. **2018,** *29*(6), 1568-1585.

[13] Koshevaya, E.; Nazarovskaia, D.; Simakov, M.; Belousov, A.; Morozov, V.; Gandalipov, E.; Krivoshapkina, E.; Krivoshapkin, P. Surfactant-Free Tantalum Oxide Nanoparticles: Synthesis, Colloidal Properties, and Application as a Contrast Agent for Computed Tomography. *J. Mater. Chem. B*. **2020,** *8*(36), 8337-8345.

[14] Mortazavi-Derazkola, S.; Salavati-Niasari, M.; Khojasteh, H.; Amiri, O.; Ghoreishi, S. M. Green Synthesis of Magnetic Fe$_3$O$_4$/SiO$_2$/HAp Nanocomposite for Atenolol Delivery and in Vivo Toxicity Study. *J. Clean Prod*. **2017,** *168*, 39-50.

[15] Al Baroot, A.; Elsayed, K. A.; Haladu, S. A.; Magami, S. M.; Alheshibri, M.; Ercan, F.; Çevik, E.; Akhtar, S.; Manda, A.; Kayed, T. S.; et al. One-Pot Synthesis of SnO$_2$ Nanoparticles Decorated Multi-Walled Carbon Nanotubes Using Pulsed Laser Ablation for Photocatalytic Applications. *Opt. Laser Technol*. **2023,** *157*, 108734.

[16] Haruna, M. A.; Nourafkan, E.; Hu, Z.; Wen, D. Improved Polymer Flooding in Harsh Environments by Free-Radical Polymerization and the Use of Nanomaterials. *Energy Fuels* **2019,** *33*, 1637-1648.

[17] Haruna, M. A; Hu, Z; Gao, H; Gardy, J; Magami, S. M; Dongshen, W. Influence of Carbon Quantum Dots on the Viscosity Reduction of Polyacrylamide Solution. *Fuel* **2019,** *248*, 205-214.

[18] Ainsworth, R. A; Crook, V; Holland, J; Magami, S. M; Norris, C. *Uv Stable Fire-Resistant Glazing Laminates*; GB Patent, 2021.

[19] Yan, L.; Xu, Z.; Wang, X. Influence of Nano-Silica on the Flame Retardancy and Smoke Suppression Properties of Transparent Intumescent Fire-Retardant Coatings. *Prog. Org. Coat.* **2017,** *112*, 319-329.

[20] Magami, S. M.; Oldring, P. K. T.; Castle, L.; Guthrie, J. T. The Effect of TiO_2, Pigmentation on the Hydrolysis of Amino Resin Crosslinked Epoxy Can Coatings. *J. Coat. Technol. Res.* **2014,** *11*, 1013-1022.

[21] Panahi, A.; Monsef, R.; Imran, M. K.; Mahdi, A. A.; Kadhim Ruhaima, A. A.; Salavati-Niasari, M. $TmVO_4/Fe_2O_3$ Nanocomposites: Sonochemical Synthesis, Characterization, and Investigation of Photocatalytic Activity. *Int. J. Hydrog. Energy* **2023,** *48*, 3916-3930.

[22] Mchedlov-Petrossyan, N. O.; Klochkov, V. K.; Andrievsky, G. V. Colloidal Dispersions of Fullerene C60 in Water: Some Properties and Regularities of Coagulation by Electrolytes. *J. Chem. Soc., Faraday Trans.* **1997,** *93*, 4343-4346.

[23] Metin, C. O.; Lake, L. W.; Miranda, C. R.; Nguyen, Q. P. Stability of Aqueous Silica Nanoparticle Dispersions. *J. Nanopart. Res.* **2011,** *13*, 839-850.

[24] Jiang, L.; Gao, L.; Sun, J. Production of Aqueous Colloidal Dispersions of Carbon Nanotubes. *J. Colloid Interface Sci.* **2003,** *260*, 89-94.

[25] Ghosh, S.; Maity, S.; Jana, T. Polybenzimidazole/Silica Nanocomposites: Organic-Inorganic Hybrid Membranes for PEM Fuel Cell. *J. Mater. Chem.* **2011,** *21*, 14897-14906.

[26] Seyedjamali, H.; Pirisedigh, A. Well-Dispersed Polyimide/TiO_2 Nanocomposites: In Situ Sol-Gel Fabrication and Morphological Study. *Colloid Polym. Sci.* **2012,** *290*, 653-659.

[27] Morimune, S.; Nishino, T.; Goto, T. Poly(Vinyl Alcohol)/Graphene Oxide Nanocomposites Prepared by a Simple Eco-Process. *Polym. J.* **2012,** *44*, 1056-1063.

[28] K., A.; Varghese, S. Role of Surfactants on the Stability of Nano-Zinc Oxide Dispersions. *Part. Sci. Technol.* **2017,** *35*, 67-70.

[29] Haruna, M. A.; Amjad, M.; Magami, S. M. Nanocomposites for Enhanced Oil Recovery. In *Emerging Nanotechnologies for Renewable Energy*; Ahmed, W., Booth, M., Nourafkan, E., Eds.; Elsevier, 2021; pp 81-113.

[30] Hu, Z.; Haruna, M.; Gao, H.; Nourafkan, E.; Wen, D. Rheological Properties of Partially Hydrolyzed Polyacrylamide Seeded by Nanoparticles. *Ind. Eng. Chem. Res.* **2017,** *56*, 3456-3463.

[31] Haruna, M. A.; Wen, D. Stabilization of Polymer Nanocomposites in High-Temperature and High-Salinity Brines. *ACS Omega* **2019,** *4*, 11631-11641.

[32] Chakraborty, S.; Panigrahi, P. K. Stability of Nanofluid: A Review. *Appl. Therm. Eng.* **2020,** *174*, 115259.

[33] Pastoriza-Gallego, M. J.; Casanova, C.; Legido, J. L.; Piñeiro, M. M. CuO in Water Nanofluid: Influence of Particle Size and Polydispersity on Volumetric Behaviour and Viscosity. *Fluid Ph. Equilibria.* **2011,** *300*, 188-196.

[34] Hu, X.; Yin, D.; Chen, X.; Xiang, G. Experimental Investigation and Mechanism Analysis: Effect of Nanoparticle Size on Viscosity of Nanofluids. *J. Mol. Liq.* **2020,** *314*, 113604.

[35] Kumar, V.; Sahoo, R. R. Viscosity and Thermal Conductivity Comparative Study for Hybrid Nanofluid in Binary Base Fluids. *Heat Transf. Asian Res.* **2019,** *48*, 3144-3161.

[36] Heijman, S. G. J.; Stein, H. N. Electrostatic and Sterical Stabilization of TiO_2 Dispersions. *Langmuir* **1995,** *11*, 422-427.

[37] Bashirnezhad, K.; Bazri, S.; Safaei, M. R.; Goodarzi, M.; Dahari, M.; Mahian, O.; Dalkılıça, A. S.; Wongwises, S. Viscosity of Nanofluids: A Review of Recent Experimental Studies. *Int. Commun. Heat Mass Transf.* **2016,** *73*, 114-123.

[38] Mahbubul, I. M.; Shahrul, I. M.; Khaleduzzaman, S. S.; Saidur, R.; Amalina, M. A.; Turgut, A. Experimental Investigation on Effect of Ultrasonication Duration on Colloidal Dispersion and Thermophysical Properties of Alumina-Water Nanofluid. *Int. Commun. Heat Mass Transf.* **2015,** *88*, 73-81.

[39] Freitas, C.; Müller, R. H. Effect of Light and Temperature on Zeta Potential and Physical Stability in Solid Lipid Nanoparticle (SLNTM) Dispersions. *Int. J. Pharm.* **1998,** *168*, 221-229.

[40] Modena, M. M.; Rühle, B.; Burg, T. P.; Wuttke, S. Nanoparticle Characterization: What to Measure? *Adv. Mater.* **2019,** *31*(32), 1901556.

[41] Haruna, M. A.; Pervaiz, S.; Hu, Z.; Nourafkan, E.; Wen, D. Improved Rheology and High-Temperature Stability of Hydrolyzed Polyacrylamide Using Graphene Oxide Nanosheet. *J. Appl. Polym. Sci.* **2019,** *136*, 47582.

[42] Haruna, M. A.; Magami, S. M. Nanoparticle Dispersions for Engineering Application. In *Science and Applications of Nanoparticles*; Jenny Stanford Publishing: New York, 2022; pp 37-45.

[43] Hao, T. Physics of Electrorheological Fluids. In *Electrorheological Fluids*; Hao, T. B., Ed.; Elsevier, 2005; pp 235-340.

[44] Chung, H. S.; Hogg, R. The Effect of Brownian Motion on Particle Size Analysis by Sedimentation. *Powder Technol.* **1985,** *41*, 211-216.

[45] Ranville, J.; Montano, M. D. Size Distributions. In *Characterization of Nanomaterials in Complex Environmental and Biological Media*; Baalousha, M., Lead, J. R., Eds.; Elsevier, 2015; pp 91-121.

[46] Corredor, L. M.; Aliabadian, E.; Husein, M.; Chen, Z.; Maini, B.; Sundararaj, U. Heavy Oil Recovery by Surface Modified Silica Nanoparticle/HPAM Nanofluids. *Fuel* **2019,** *252*, 622-634.

[47] Corredor-Rojas, L. M.; Hemmati-Sarapardeh, A.; Husein, M. M.; Dong, M.; Maini, B. B. Rheological Behavior of Surface Modified Silica Nanoparticles Dispersed in Partially Hydrolyzed Polyacrylamide and Xanthan Gum Solutions: Experimental Measurements, Mechanistic Understanding, and Model Development. *Energy Fuels* **2018,** *32*, 10628-10638.

[48] Jiang, T.; Kuila, T.; Kim, N. H.; Lee, J. H. Effects of Surface-Modified Silica Nanoparticles Attached Graphene Oxide Using Isocyanate-Terminated Flexible Polymer Chains on the Mechanical Properties of Epoxy Composites. *J. Mater. Chem. A* **2014,** *2*, 10557-10567.

[49] Haruna, M. A.; Gardy, J.; Yao, G.; Hu, Z.; Hondow, N.; Wen, D. Nanoparticle Modified Polyacrylamide for Enhanced Oil Recovery at Harsh Conditions. *Fuel* **2020,** *268*, 117186.

[50] Rutnakornpituk, M.; Thompson, M. S.; Harris, L. A.; Farmer, K. E.; Esker, A. R.; Riffle, J. S.; Connolly, J.; St. Pierre, T. G. Formation of Cobalt Nanoparticle Dispersions in the Presence of Polysiloxane Block Copolymers. *Polymer (Guildf)* **2002,** *43*, 2337-2348.

[51] Jang, H.; Lee, W.; Lee, J. Nanoparticle Dispersion with Surface-Modified Silica Nanoparticles and Its Effect on the Wettability Alteration of Carbonate Rocks. *Colloids Surf. A. Physicochem. Eng. Asp.* **2018,** *554*, 261-271.

[52] Maurya, N. K.; Mandal, A. Studies on Behavior of Suspension of Silica Nanoparticle in Aqueous Polyacrylamide Solution for Application in Enhanced Oil Recovery. *Pet. Sci. Technol.* **2016,** *34*, 429-436.

[53] He, Y.; Jin, Y.; Chen, H.; Ding, Y.; Cang, D.; Lu, H. Heat Transfer and Flow Behaviour of Aqueous Suspensions of TiO2 Nanoparticles (Nanofluids) Flowing Upward through a Vertical Pipe. *Int. J. Heat Mass Transf.* **2007,** *50*, 2272-2281.

[54] Nguyen, C. T.; Desgranges, F.; Roy, G.; Galanis, N.; Maré, T.; Boucher, S.; Angue Mintsa, H. Temperature and Particle-Size Dependent Viscosity Data for Water-Based Nanofluids-Hysteresis Phenomenon. *Int. J. Heat Fluid Flow* **2007,** *28*, 1492-1506.

[55] Godson, L.; Raja, B.; Lal, D. M.; Wongwises, S. Experimental Investigation on the Thermal Conductivity and Viscosity of Silver-Deionized Water Nanofluid. *Exp. Heat Transf.* **2010,** *23*, 317-332.